

VIBRATION FIELD PROBLEM RESOLVED WITH ANALYTICAL DIAGNOSTICS APPROACH AND INNOVATIVE IMPELLER DESIGN

by

Bruno Schiavello

Director for Fluid Dynamics

Flowserve Pump Division

Applied Technology

Phillipsburg , New Jersey

and

Giancarlo Cicatelli

Hydraulic Specialist

Flowserve Pump Division

Desio, Milan, Italy



Bruno Schiavello has been Director for Fluid Dynamics at Flowserve Pump Division, Applied Technology Department, in Phillipsburg, New Jersey, since 2000, and previously served in the same position with Ingersoll Dresser Pump Company. He started in the R&D Department of Worthington Nord (Italy), joined Central R&D of Worthington, McGraw Edison Company, and then Dresser Pump Division.

Mr. Schiavello was co-winner of the H. Worthington European Technical Award in 1979. He has written several papers and lectured at seminars in the area of pump recirculation, cavitation, and two-phase flow. He is a member of ASME, has received the ASME 2006 Fluid Machinery Design Award, and has served on the International Pump Users Symposium Advisory Committee since 1983.

Mr. Schiavello received a B.S. degree (Mechanical Engineering, 1974) from the University of Rome, and an M.S. degree (Fluid Dynamics, 1975) from Von Karman Institute for Fluid Dynamics.



Giancarlo Cicatelli has been Hydraulic Specialist at Flowserve Pump Division since 2000, and is a member of the Corporate Technology group. He is based in Desio, Milan, Italy. Dr. Cicatelli's principal fields of interest are focused on the fluid dynamic of turbomachines, with specific attention to the design, development, and testing of centrifugal pumps and pumping systems. He is author

of several scientific publications in the field of fluid dynamics applied to turbines and pumps.

Dr. Cicatelli has a B.S. degree (Aeronautical Engineering) from the University of Naples, an M.S. degree from the von Karman Institute, and a doctoral degree (Applied Sciences) from the von Karman Institute and the Université Libre de Bruxelles–Belgium. He worked at the von Karman Institute as a research assistant and as a research associate at the University of Cambridge in the field of the fluid dynamics of turbomachinery. He is a chartered professional engineer.

ABSTRACT

Several pump units of the same design installed in various locations in the USA with different duties exhibited high vibrations above API limits with process fluids ($SG = 0.5$ to 0.6) from rated point down to minimum continuous flow.

The investigation for root cause was conducted along two parallel paths: experimental and theoretical. On the experimental side a series of shop vibration tests and modal analysis was carried out at full operational speed and cold water ($SG = 1.0$). These tests included: pump as installed and two modifications of the bearing housings. With the theoretical approach several computer codes of hydraulic analysis were used for analytical diagnosis in order to identify the internal hydraulic phenomena inducing the vibrations. Unsteady hydraulic forces, very likely associated with impeller discharge recirculation, were eventually considered to produce the hydraulic excitation for high vibrations.

The strategy for the ultimate solution was based on a new hydraulic design impeller with innovative geometry, i.e., two blade rows with five vanes at inlet and nine vanes at outlet. Shop tests at full operational speed confirmed both the expected pump curve and presented vibrations levels (overall and vane pass) drastically reduced below API limits in the whole operating range, from rated flow down to minimum continuous flow. The new impeller was installed in all sites keeping the existing bearing housings. Field vibration data with the new impeller were collected at different times in a one year period and are compared with data produced by the old impeller. The field vibration levels with the new innovative impeller have been drastically reduced for both the overall amplitude and at vane pass frequency. The key hydraulic design parameter appears to be a high number of vanes at the impeller outlet.

INTRODUCTION

Field Vibration Problem

During 2004 a common vibration problem was experienced in four different plants (refineries) in the USA with the same pump type/size operating apparently with different conditions of services. The pump type/size is an API 6 inch discharge pump with top-top configuration, double suction impeller, double volute, antifriction bearings configuration, center mounted (BB2). The cross section of the pump is given in Figure 1 and two cut views are shown in Figure 2. The pump overall characteristics at design speed ($N_{des} = 3565$ rpm) and impeller maximum diameter ($D_{2des} =$

19.09 inch) are given in Figure 3. The best efficiency point (BEP) is at $Q_{BEP} = 3100$ gpm and $H_{BEP} = 1490$ ft, which give a specific speed $N_S = 828$ US (using total flow). Moreover: $NPSHR_{BEP} = 30$ ft, which gives a suction specific speed $S_{eye} = 10,950$ US (using half capacity). The impeller has five vanes and an eye diameter $D_{eye} = 6.4$ inch. The nominal operating speed at site is $N_{oper} = 3545$ rpm for all pumps, which gives a peripheral eye velocity $U_{eye} = 99.0$ ft/s. The key operating data at rated capacity for each installation are presented in Table 1 and also shown in Figure 3. The impellers are trimmed with different duty diameter (Table 1). The diameter of the two volute cutwaters is the same for all four cases with $D_3 = 20.51$ inch.

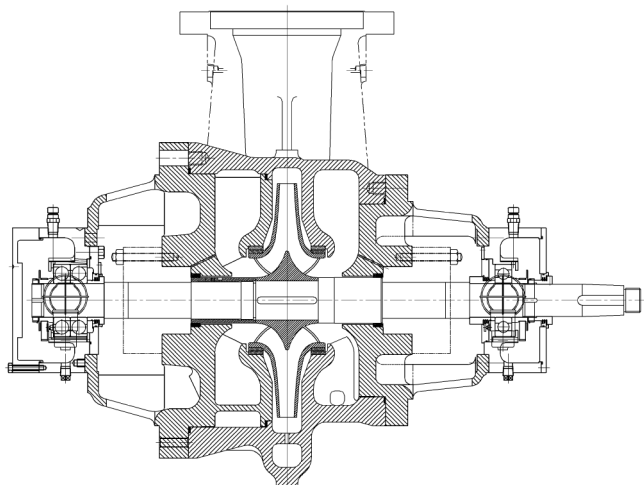


Figure 1. Pump Cross Section.

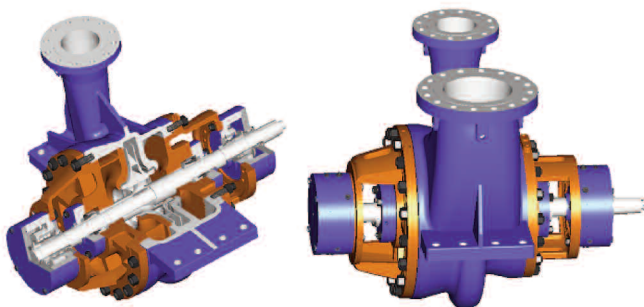


Figure 2. Pump Cut Views.

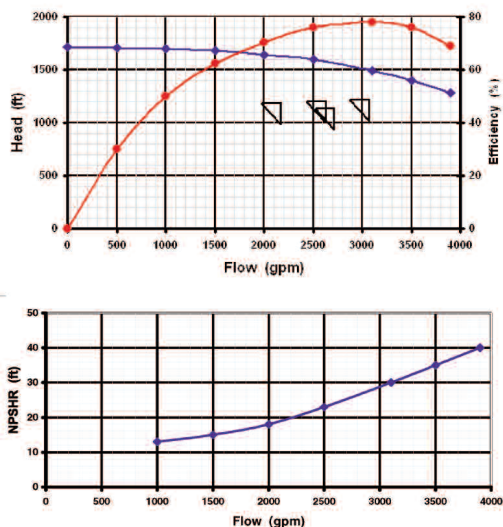


Figure 3. Pump Curve Characteristics.

Table 1. Key Operating Data at Rated Capacity (Contractual).

Case N.	1	2	3	4
Q (gpm)	2720	3070	2176	2634
H (ft)	1136	1218	1181	1200
D2 (in)	16.73	17.72	16.93	17.32
SG	0.569	0.560	0.724	0.735
MCSF (gpm)	671	1000	917	942
NPSHR (ft)	24.3	29.5	19.2	23.4
NPSHA (ft)	39	35	30.6	52.4
N. of units	2	2	2	2

For Case 1 and 2 the level of bearing vibration at site with actual fluid (SG = 0.569 and 0.560) was exceeding the API limit 0.12 ips overall. These two pumps were tested in the shop at 2950 rpm (in 2002 to 2003) with cold water (SG = 1.0) and did not show any critical vibration level. In two cases (Case 3 and 4) the pumps were installed (Figure 4) but not yet operated and the solution that was identified and herein described was later implemented as a preventive action. For Case 1 and 2 the highest overall level at site (Figure 5) was at the drive end (DE) (DEV slightly higher than DEH) from 0.16 up to 0.45 ips at rated capacity. Experience was suggesting that further increasing vibrations could be expected below the rated flow toward minimum continuous stable flow (MCSF) (contractual value: 1000 gpm). The analysis of the vibration spectra clearly pointed out:

- Dominant vane pass frequency (around 300 Hz, five vanes)
- Relevant contribution of low frequencies in a broad band range

It is worthy noticing that the B gap ($= 1 - D_3/D_2$ duty) for Case 1 and 2 is 22 percent and 16 percent, respectively.



Figure 4. The Pump in the Field (Case 4).

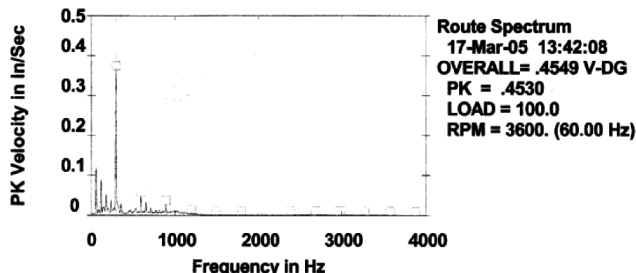


Figure 5. Field Vibration Spectra at DEV (Case 2, $Q_{rated} = 3070$ gpm).

Insights from Background Literature

The above vibration aspects associated to both rated capacities below design capacity, and marginal NPSHA/NPSHR (especially Case 2), suggest that the high vibrations can be caused by one or more of the following physical mechanisms, either acting separately or mutually interacting.

Flow Recirculation at Impeller Inlet (Suction Recirculation) and/or at Impeller Outlet (Discharge Recirculation)

The triggering mechanism of the suction recirculation is flow separation at tip blade leading edge on suction side due to high incidence angle and/or high vane loading when the impeller is operating at part capacity below the shockless flow (Schiavello, 1982; Schiavello and Sen, 1980 and 1981). The flow on the blade suction side becomes very unsteady as shown by flow visualization (Minami, et al., 1960; Barrand, et al., 1984). By slight reduction of the capacity a peculiar flow pattern like rotating stall with subsynchronous frequency is observed at the impeller inlet (Sen, et al., 1979; Breugelmans and Sen, 1982). This capacity is usually called "Suction Recirculation Onset Capacity." With further reduction of the capacity a full annular flow pattern with reverse axial velocity and also tangential velocity (prerotation) is settled at the impeller inlet with increasing intensity (Schiavello and Sen, 1980 and 1981) causing pressure pulsations at impeller inlet with broadband frequency spectrum (Breugelmans and Sen, 1982; Sloteman, et al., 1984). The onset of the "discharge recirculation" has been related with a sudden increase of the pressure pulsations at the pump discharge (Fraser, 1981). Direct experimental detection is not well documented in literature (Barrand, et al., 1984). Presently it is not clear if the triggering mechanism is related to the impeller geometry only (Fraser, 1981) or volute cutwaters/vaned diffuser geometry (Hergt and Starke, 1985) or to both aspects. It may be suspected that the onset of discharge recirculation is flow separation at the impeller outlet due to high local vane loading and possibly upstream effect of the volute/vaned diffuser. A peculiar aspect seems to be a sharp increase of the pressure pulsations at vane passage frequency (VPF) at impeller outlet (Barrand, et al., 1984), which could be associated with the formation of large wakes at the outlet of each blade passage caused by flow separation. Shop tests show in several cases a sudden increase of the bearing housing vibrations (radial components) at VPF for a capacity below the best efficiency point. Moreover, the unsteadiness of these wakes causes pressure pulsations and vibrations characterized by a broadband frequency spectra. Shop and field data of vibrations at pump bearing housing with low flowrates (certainly in presence of suction recirculation/discharge recirculation) present increasing amplitude levels with decreasing capacity along with broadband frequency spectra (from 10 to 20 Hz to 500 to 1000 Hz).

Cavitation–Suction Recirculation Interaction

Pump operating within a capacity range around the impeller shockless flow (roughly close to BEP Capacity at impeller outlet diameter design) with NPSHA below NPSHinc (inc = inception, i.e., no vapor bubbles at all) are subjected to a cavitation pattern characterized by a vapor pocket attached to the blade surface near the leading edge (Cavitation Mode called "blade attached cavitation" or "sheet cavitation") (Minami, et al., 1960; Güllich, 1989; Schiavello, 1993). This cavitation mode is present in almost all pump services using current NPSHA margins, which are traditionally and simply based on NPSHR (typically: NPSHA/NPSHR from 1.1 to 1.5 except for high energy pumps like boiler feed pumps and/or high speed pumps). In this regime the cavitation is alone and is characterized by collapse of vapor bubbles that cause an increase of pressure pulsations above the background level with wide frequency spectra (from 100 Hz to 180

KHz, approximately) (Kercan and Schweiger, 1979; Schiavello, 1982; Güllich, 1989; Cooper, et al., 1991; Florjancic, et al., 1993). The effect in terms of bearing vibrations frequency spectra is not uniquely defined although the main aspect seems to be a broad band spectrum from 100 Hz to 2000 Hz (Bolleter, et al., 1991; Florjancic, et al., 1993).

At low flow rates when suction recirculation is also present, then a new cavitation mode can be present called "vortex cavitation" (Okamura and Miyashiro, 1978; Schiavello, 1993). In this regime of capacities and NPSHA (with usual margins above NPSHR) the flow pattern at the impeller inlet is complex and very unsteady with alternation of cavitation alone (as vertical rope from the suction side of one blade to the pressure side of the adjacent blade) and suction recirculation alone (as described above). This unsteady flow mechanism of cavitation-suction recirculation interaction completely confined within the pump causes pressure pulsations both at impeller suction (Sloteman, et al., 1984; Cooper, et al., 1991) and discharge (Kawata, et al., 1984), which lead to dynamic radial loads (Kawata, et al., 1984) and vibrations (Cooper, et al., 1991). The maximum unsteadiness (as indirectly shown by the amplitude of pressure pulsations (Cooper, et al., 1991) and dynamic radial loads (Kawata, et al., 1984) are occurring at NPSHA level between NPSHinc (dominating suction recirculation) and NPSHR (dominating cavitation). The frequency spectra (suction pressure pulsations and vibrations) have a spread band typically below 1000 Hz (Sloteman, et al., 1984; Cooper, et al., 1991). (*Note:* This phenomenon is different from surge, which is an interaction between the pump and the circuit.)

Strong Impeller-Volute Interaction

The pattern of the relative velocity around the impeller exit is not uniform but periodic with as many flow streams as the number of blade passages. Each flow stream is characterized by an angular zone with high velocity and an adjacent zone with small velocity or even zero velocity (corresponding to the blade tangential thickness). The angular gradients of relative velocity within each stream exist even at BEP (with smallest values) and increase at capacities away from the BEP. The angular pattern of the static pressure around the impeller periphery has a similar aspect (periodic with internal gradients). The periodic-distorted pattern of both the relative velocity and static pressure rotate with the impeller. There is a mixing process occurring within the radial gap between the impeller exit and volute cutwaters or vaned diffuser blade leading edge (B gap), which reduces the distortion of the periodic flow and even produces a full uniform flow (at BEP with large B gap). In general with conventional design B gap (6 to 10 percent with double volutes) the mixing process is not fully completed, particularly at part flows. Then the interaction with the rotating periodic-distorted flow pattern and the stationary vanes (volute cutwaters/diffuser vanes) generates pressure pulsations with periodic character with fundamental frequency equal to impeller vane passage (VPF) and other harmonics, depending on the number of volute cutwaters/diffuser blades (Bolleter, 1988; Güllich and Bolleter, 1992). The amplitude of the pressure pulsations at BEP and part flows (always increasing with reducing capacity) depends on various design parameters related with the geometry of both the impeller outlet and volute cutwaters/diffuser blades (Domm and Hergt, 1970; Kanki, et al., 1981; Makay and Barrett, 1984; Güllich, et al., 1987; Robinett, et al., 1999). These pressure pulsations induce vibrations at VPF (Robinett, et al., 1999). The key character is that below the pump BEP, the amplitude of pressure pulsations and bearing vibrations at VPF is increasing while the flow is decreasing (Kanki, et al., 1981; Güllich, et al., 1987; Verhoeven, 1987; Florjancic and Frei, 1993).

Highly Unsteady Flows Linked with High Vane Loading

The impeller vane loading is given by the distribution of the relative velocity (and pressure) around the blade surface from

leading edge to the trailing edge. Two aspects are important in relation to the generation of flow unsteadiness (and stability):

- The ratio (Wss-Wps)/Waverage at each blade location, which defines the local loading, and
- The gradient of Wss (or Wps) along the chord, which is strictly related with the diffusion process of the relative velocity.

These two parameters along the curvature of the blade channel (both along the impeller tip-hub and the blade surfaces) govern the formation of secondary flows and boundary layers growth inside the blade channel, which in turn determine the level of flow unsteadiness and associated pressure pulsations. Also the flow turbulence is associated with these vane loading parameters. Typically the amplitude of flow unsteadiness and level of turbulence become stronger with impeller vane loadings, i.e., with high values of the above parameters, due to a design choice (impeller geometry selection) and/or pump duty at part flow away from BEP capacity (Kauptert and Staubli, 1999a, 1999b). The frequency spectra (pressure pulsations and pump bearing vibrations) associated with such internal flow mechanisms are supposed to have broadband range from 10 Hz to 1000 Hz, by indirect analogy with experimental observation with piping elbows and diffusers (Eisele, et al., 1997).

Structural Response of Bearing Housing at 3565 RPM

The structural vibration modes of the bearing housing (natural frequencies and corresponding damping factors) are an essential factor in determining the amplitude levels of vibrations in presence of internal hydraulic excitation mechanisms (Verhoeven, 1987 and 1988, Florjancic and Frei, 1993). This is in general a “forced vibration” situation, where the excitation frequency can be the VPF or other characteristic frequency of the internal hydraulic source (e.g., rotating stall, suction recirculation, flow turbulence).

ROOT CAUSE INVESTIGATION

Experimental Investigation—Shop Tests

In the summer of 2004 a series of shop vibration tests with cold water, SG = 1.0, was carried out with the aim of gaining insights under controlled operating conditions (including ample NPSHA and also simulation of field suction piping), which would help to identify the root cause. The main scope of shop tests was to identify possible factors linked with the mechanical design of the bearing housings and particularly their structural response at the design speed of 3565 rpm (close to the field operating speed, $N_{oper} = 3545$ rpm). Case 4 was selected as reference, also considering the urgent needs of the end user.

The first test was a baseline test with the pump as-built and installed, i.e., original design of bearing housings and also trimmed impeller diameter. The vibrations (overall levels and spectra) were measured at five capacities, including the pump design capacity and other flows within the expected field operating range (from rated to MCSF). The vibration spectra for two capacities (1750 gpm indicative of the pump behavior at part flow and 2690 gpm close to the rated one) are shown in Figures 6 and 7, respectively (vibrations level are shown in mm/s = 25.4 × ips). The fundamental frequency 1× is at 59.4 Hz = 3565 cpm and the vane pass frequency 5× is at 297 Hz = 17,825 cpm (VPF). These characteristic frequencies are evident for both capacities, particularly the VPF, with different levels for each vibration component (DE = drive end, NDE = nondrive end, H = horizontal, V = vertical, A = axial). One peculiar aspect common to both spectra is the presence of vibrations in a very broad band range up to 55,000 cpm (917 Hz). This peculiar aspect is exhibited by all the spectra in the whole flow range, even at the design capacity. From literature data, it can be associated with the presence of pressure pulsations caused by suction/discharge recirculation (Sen, et al., 1979; Breugelmanns and Sen, 1982; Sloteman, et al., 1984).

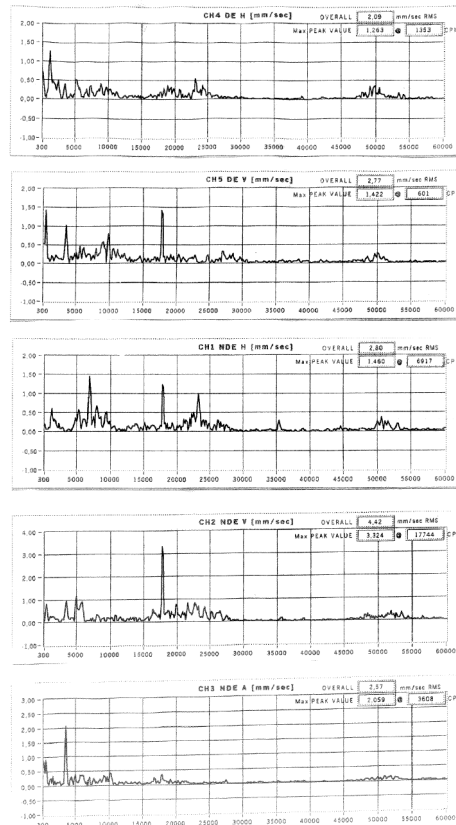


Figure 6. Shop Test Spectra at 1750 GPM.

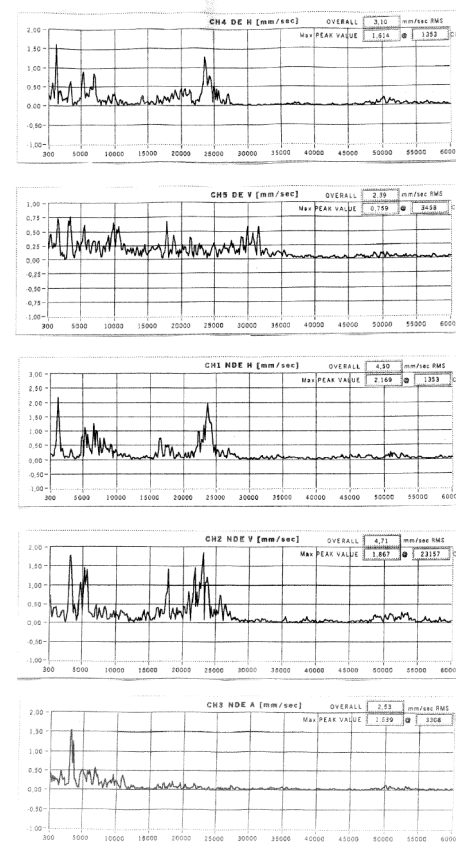


Figure 7. Shop Test Spectra at 2690 GPM.

The trend of vibration levels (overall, 1×, and 5× or VPF) versus capacity is shown in Figures 8, 9, and 10. It is evident that the overall level exceeds the vibration limits of 0.12 ips (preferred operating range) and 0.15 ips (allowable operating range, including MCSF) for the DE bearing housings, especially for the vertical component, which is high in the full capacity range, from design flow down to MCSF. Also the 1× and VPF are high for DEV.

Basically the shop vibration data (amplitude and spectra) with cold water reproduced at different level the field vibration characteristics at the same speed but different fluid density (SG = 0.56) and different speed of sound. This observation clearly indicated that the source of vibration was not related to a physical excitation like acoustic resonance (either related with the pump internal geometry or induced by a pump-system interaction). Rather the source of vibrations appeared inherent with the pump design, hydraulic and/or mechanical.

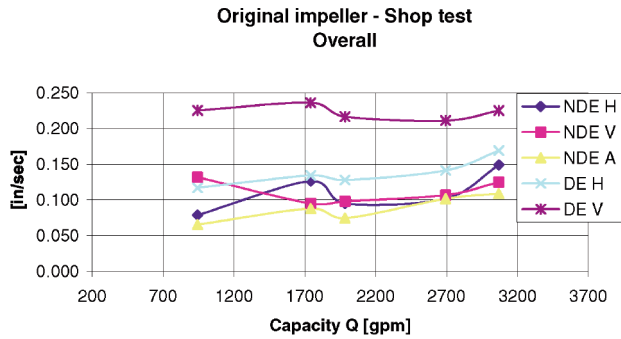


Figure 8. Shop Test Vibration Readings—Overall.

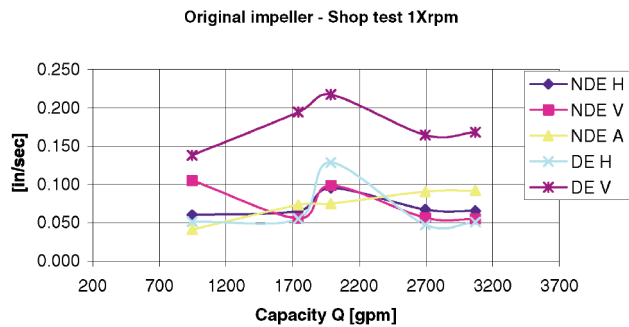


Figure 9. Shop Test Vibration Readings—1× RPM.

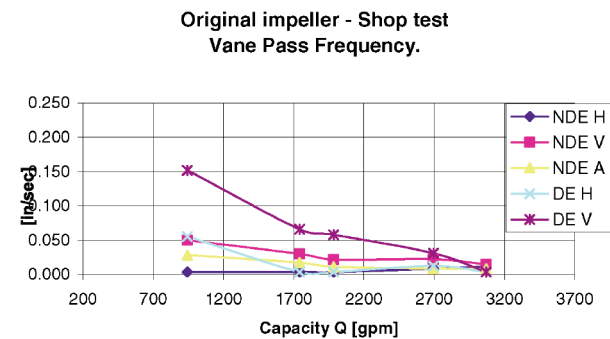


Figure 10. Shop Test Vibration Readings—Vane Pass Frequency.

An experimental modal analysis was performed in order to determine the structural response of the pump and particularly identify possible resonance frequencies of the bearing housings. A hammer test was performed with the pump suspended in the air to avoid superposition of stand effects. The transfer function of the signal measured on each bearing housing in the horizontal and vertical position is illustrated in Figure 11. Then the following natural

frequencies (Table 2) appeared to be close to the VPF frequency (297 Hz) for both the DE and NDE bearing housings (first natural frequency). An attempt to modify the resonance characteristics of the pump bearing housings was performed by adding selective mass to each bearing housing. The corresponding transfer function of the signal measured on the bearing housing in the horizontal and vertical position is illustrated in Figure 12. The associated natural frequencies are indicated in Table 3. It appears that all the first natural frequencies were only marginally shifted to lower values, still remaining close to the VPF. However the vibrations were measured to see whether the pump under running conditions would show any improvement. The trend of vibration levels (overall, 1×, and 5× or VPF) versus capacity is shown in Figures 13, 14, and 15. The vibrations were reduced for the DE bearing housing, but increased for the NDE one, in agreement with the new natural frequencies.

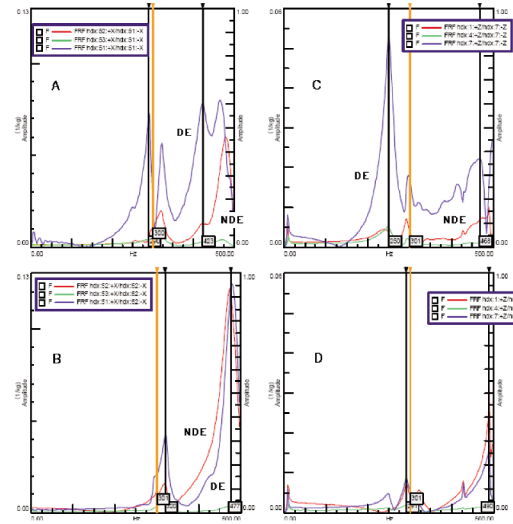


Figure 11. Modal Analysis—Pump in the Original Configuration.

Table 2. Natural Frequencies (Original Pump Suspended).

	Natural frequency [Hz]	
	DE	NDE
HORIZONTAL	290	320
	423	477
VERTICAL	250	291
	468	490

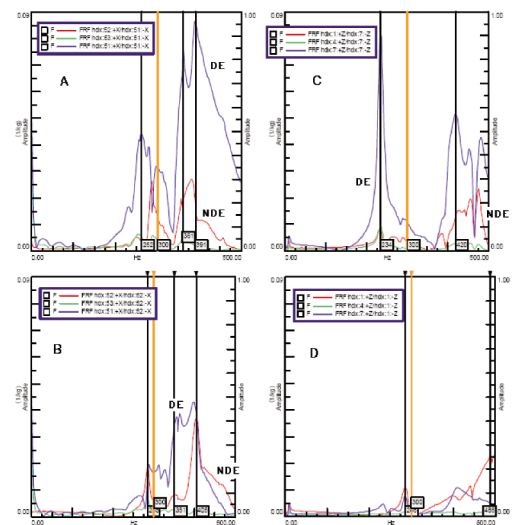


Figure 12. Modal Analysis—Pump with Modified Configuration.

Table 3. Natural Frequencies (Modified Pump Suspended).

	Natural frequency [Hz]	
	DE	NDE
HORIZONTAL	262-300	285
	361-391	405
VERTICAL	234	286
	420	488

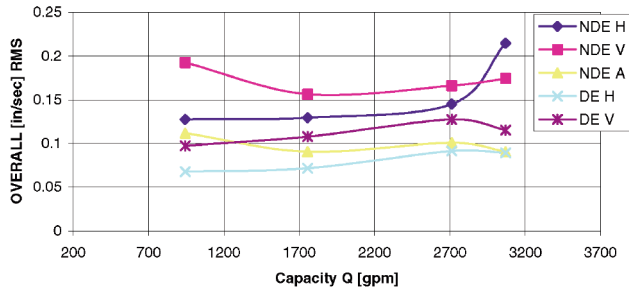


Figure 13. Shop Test—Modified Pump—Overall.

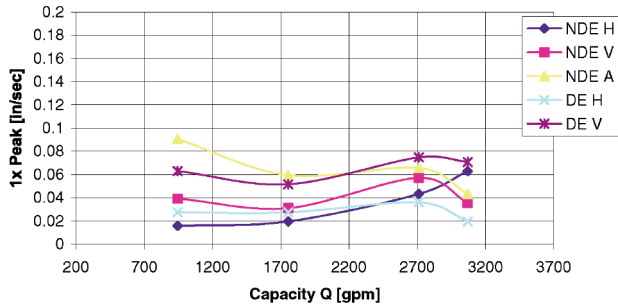


Figure 14. Shop Test—Modified Pump—1x RPM.

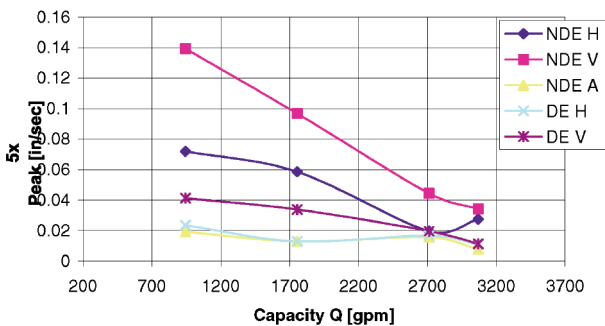


Figure 15. Shop Test—Modified Pump—Vane Pass Frequency (Mass Added to the Bearing Housings).

The approach of lowering the natural frequencies by adding mass to the bearing housing seemed promising and a new attempt was made in the same direction by using a greater mass for the NDE one. There was only some improvement but the overall vibrations and VPF for NDEV at lower capacities (including MCSF) remained higher than API limit. These modifications of the bearing housings, which produced partial improvements near the rated capacity, were envisaged as possible short term solutions with limitations of the pump operating range.

Analytical Diagnostic Approach

A thorough hydraulic analysis was conducted as an independent complementary diagnosis path for identifying the hydraulic excitation source of the vibrations, which was clearly suggested by two peculiar aspects:

- Flow dependence, and
- Broadband frequency spectra.

This theoretical investigation was aimed at finding the dominant factor (true root cause) and determining the ultimate solution. The approach included several hydraulic criteria:

- Step 1—Off-design criteria: evaluation of Q_{rated}/Q_{BEPmax} and $Q_{rated}/Q_{BEPduty}$.
- Step 2—Determination of impeller-volute matching capacity (optimum capacity with minimum static and dynamic radial load). The scope is to get a preliminary clue about possible strong interaction between volute and impeller (with geometry at duty diameter). An internal computer code was used, which is based on the theory developed by Worster (1960, 1963).
- Step 3—First determination of onset capacity for suction recirculation (Q_{rs}) and discharge recirculation (Q_{rd}). Analytical tool: empirical correlation published by Fraser (1981).
- Step 4—Verification of Step 3 with full analysis of existing impeller including various criteria (Schiavello and Sen, 1980), i.e., diffusion ratio, inlet incidence angle, overall vane loading, meridional area progression. Analytical tool: internal computer code.

Some key results of the analysis are summarized in Table 4.

Table 4. Hydraulic Analysis—Indicative Results.

	CASE 1	CASE 2	CASE 3	CASE 4
Grated / Q _{bep-max}	0.90	1.02	0.72	0.87
Grated / Q _{bep-duty}	1.00	1.06	0.8	0.87
Grated / Q _{rs}	1.10	1.24	0.87	1.06
Grated / Q _{rd}	0.96	1.03	0.77	0.90
D3 / D2duty	1.22	1.16	1.21	1.18

The above data (in addition with other results) pointed out that the “discharge recirculation” was very likely the root cause of high overall vibrations at rated flows and below, particularly in relation to vane passage frequency. Further field investigation for Case 2 indicated that the actual field capacity (field vibration measurements refer to this case) was 2380 gpm, i.e., $Q_{actual}/Q_{rd} = 0.8$ (and even $Q_{actual}/Q_{rs} = 0.95$). Moreover, the contribution from volute interaction to vane pass vibration appeared secondary due to large clearance between the volute cutwaters and the impeller outlet (B gap = 16 percent from Table 4) (Robinett, et al., 1999). This indicated that the discharge recirculation triggering mechanism was in this case mainly related with the impeller design leading to early and strong discharge recirculation.

Thus the vibration problem was recognized as primarily a case of “forced vibrations” excited by hydraulic forces at the impeller outlet caused by flow separation (high vane loading) usually named “discharge recirculation.” The unsteady flows associated with flow separation at impeller outlet (“discharge recirculation”) generate high pressure pulsation with broad frequency range apart from vane pass frequency and induce vibrations with many frequencies as shown by the frequency spectra even at rated flow. The presence of these frequencies raise the overall vibration levels. The presence of first natural frequency in each bearing housing observed in the baseline shop test (original design) is surely a contributing factor, mainly responsible for relatively high amplitudes at VPF in some vibration components.

**SOLUTION STRATEGY—
INNOVATIVE IMPELLER GEOMETRY**

A new design impeller was considered as the most effective first step of a solution strategy with high probability of success. Additional corrective steps (bearing response change, cutwaters modifications, operating range restrictions) were considered only as backup steps.

The impeller design strategy was focused on the following criteria (with decreasing ranking from top A):

- Delay the discharge recirculation onset capacity below lowest rated flow (Case 3), i.e., $Q_{rated}/Q_{BEPduty}$ (rank A)
- Reduce the discharge recirculation strength (energy level of the exciting hydraulic forces or dynamic radial loads) (rank A)
- Change the impeller vane number to reduce vane loading, pressure pulsations, and move away from possible natural frequency of DE bearing (increased number of vanes) (rank A)
- Reduce the suction recirculation onset capacity and strength (rank A)
- Keep or increase volute cutwater-impeller clearance, i.e., keep or reduce impeller duty diameter (rank A)
- Keep rated flow and head (rank A)
- Maintain efficiency at rated flow close to contractual value within maximum negative deviation of 1 point (rank A/B)
- Revise and marginally increase MCSF for each case thus redefining the lower end of the operating range within API vibrations limit (rank B)

The above design requirements led to conflicting choices for the vane geometry (number and shape) between the inlet and outlet of the impeller geometry. Then an innovative impeller geometry was selected with a double row of vanes (Schiavello, et al., 1997). The solid model of this impeller, which also represents the master pattern, is shown in Figure 16 (front view) and Figures 17 and 18 (top view, outboard and inboard), which presents the key elements, i.e., first blade row (red), second blade row (brown), central rib (green), and one shroud (gray). The vanes are not staggered at the exit because of small impeller width that would prevent cleaning of casting. Moreover, a full diameter central rib would drastically impair the efficiency.

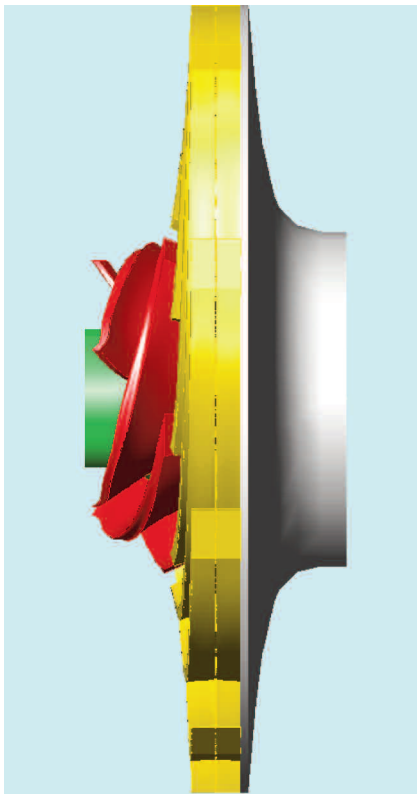


Figure 16. New Design Impeller (Side View).

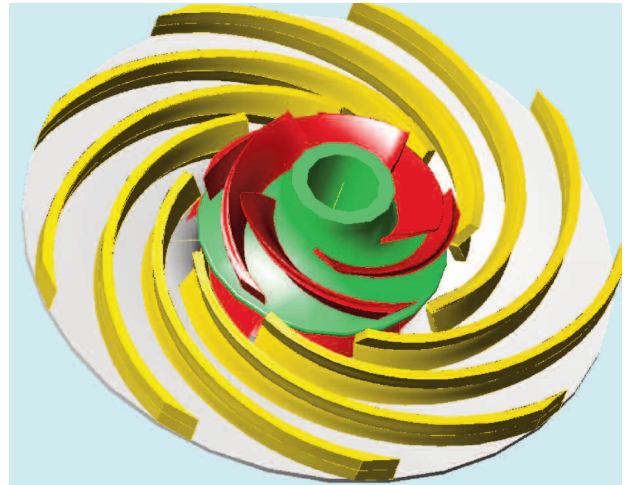


Figure 17. New Design Impeller (Front View—Outboard).

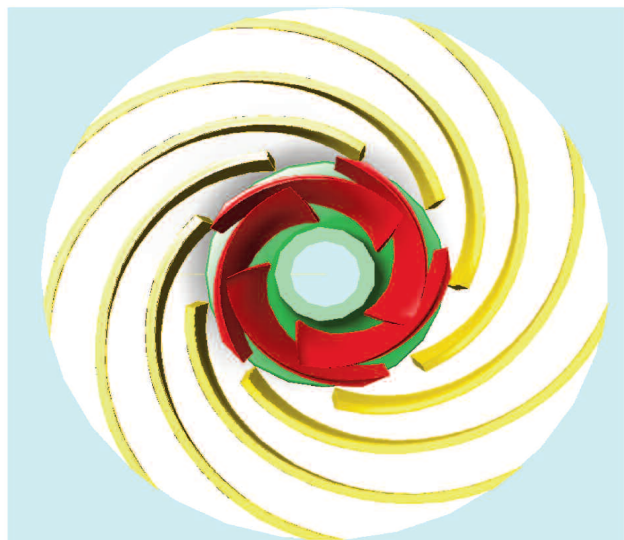


Figure 18. New Design Impeller (Front View—Inboard).

An internal computer code for pump hydraulic design, which incorporates theoretical one-dimensional fluid model for various hydraulic losses, was used as an analytical tool to optimize the impeller geometry by evaluating several variants through the same sequence of the above steps (with specific computer codes) applied for the diagnostic stage. The number of vanes for second row (Z_2) represented the key design parameter controlling the discharge recirculation onset capacity ratio. This could be reduced below rated capacities only going to high number of vanes at exit, i.e., the analysis showed that: $Q_{rd}/Q_{BEPduty} = 0.7/0.75/0.80$ for $Z_2 = 10/9/8$ (Z_2 = number of vanes for the second row) with increasing impeller efficiency. The compromise choice for impeller vane number configuration was selected to be 5 + 9, which fits correctly with double volute.

The selection of a high number of vanes for the impeller outlet is also very effective for minimizing the interaction with the volute cutwaters and reducing the amplitude of the pressure pulsation at VPF (Timouchev and Tourret, 2002). These pressure fluctuations are present at the impeller outlet and generate dynamic radial hydraulic forces at VPF, which are directly responsible for radial vibrations at VPF and increase at off-design, particularly at part flows (namely MCSF).

The computer software for hydraulic design generate several output formats for geometry evaluation and manufacturing. Some

output electronic files are used for automatic generation of the impeller hydraulic layouts and also the corresponding solid model (Figures 16, 17, and 18). The impeller solid models were created for various impeller variants, which were used for evaluating the manufacturing feasibility/constraints with pattern maker, foundry, and machine shop. The impeller castings were made by using a conventional ceramic core process.

RESULTS

Shop Performance and Vibration Data

The shop test with the new design impeller was first performed with the impeller maximum diameter (also design: $D_{2des} = 19.09$ inch) and showed that the BEP flow and head were slightly increased (+ 2 percent) and the efficiency was within tolerance. The NPSHR was maintained with Seye of 10,900. The discharge recirculation onset capacity was lowered ($Q_{rd}/Q_{BEPmax} = 0.75$ from 1.04). Also the suction recirculation onset capacity was delayed ($Q_{rs}/Q_{BEPmax} = 0.60$ from 0.82). Then the pump reliability at part flow was enhanced without a relevant sacrifice of overall performance.

The vibration shop test (3565 rpm, SG = 1.0—cold water) revealed a drastic reduction of all vibration components below API acceptance limits keeping the original design bearing housings (DE and NDE). The trend of these vibration levels versus capacity is shown in Figures 19, 20, and 21. The overall vibration level (Figure 19) was markedly reduced for all components, particularly for DE-bearing (by a factor 3 or plus) and brought within API limit. The Figure 20 presents the vibration level at the synchronous frequency $1 \times rpm$ for all components (at DE and NDE) in the full operating range. It appears that this frequency (largely influenced by mechanical rotor unbalance) gives the major contribution to the overall amplitude. Moreover the relation with capacity for each component is very similar between $1 \times rpm$ and overall level, showing limited and even irregular change (second order). The vibration levels at vane pass frequency for exit vane number (new impeller $Z_2 = 9$, VPF = 531 Hz) resulted nearly negligible (Figure 21) and well below the API limit of 0.08 ips in the whole operating range from BEP capacity down to MCSF. It is worthy noticing that the B gap for this shop test was 7.2 percent. Also the shop vibration spectra showed very low level at 5 V frequency (297 Hz), which is the VPF for the first row of blades from BEP to MCSF.

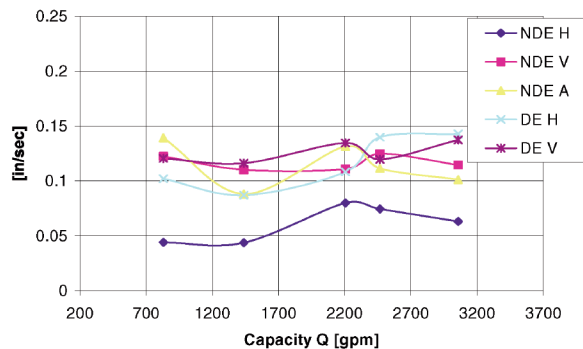


Figure 19. Shop Test—New Design Impeller—Overall.

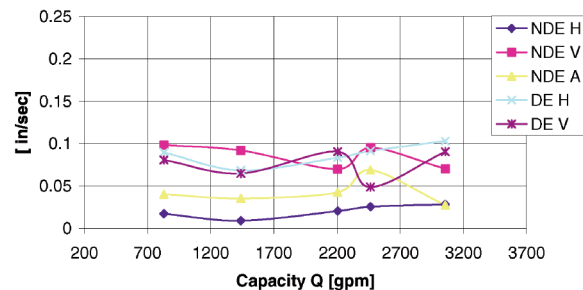


Figure 20. Shop Test—New Design Impeller—1x RPM.

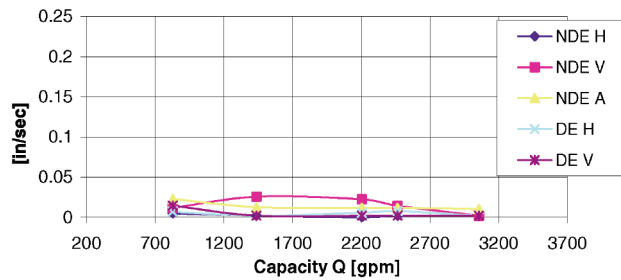


Figure 21. Shop Test—New Design Impeller—Vane Pass Frequency.

One shop vibration frequency spectrum with the new impeller is shown in Figure 22 for the capacity of 2690 gpm (close to rated one), which is also indicative for the other capacities. The corresponding shop vibration frequency spectrum with the old impeller is shown in Figure 7. By comparison it appears that the bandwidth of frequencies with peaks below $0.5 \text{ mm/s} = 0.02 \text{ ips}$ is reduced by a factor 2 for each vibration component.

Moreover the frequency activity is negligible with the new design impeller above 250 Hz (15,000 cpm) compared to 550 Hz (35,000 cpm) for the old design impeller.

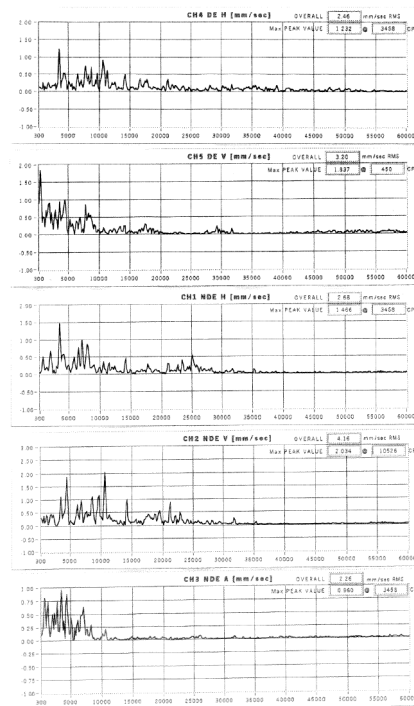


Figure 22. Shop Test Spectra at 2690 GPM—New Impeller.

In synthesis the shop data clearly revealed that the vibration levels were much lower with the new impeller and also presented a nearly flat trend in a wide capacity range (from above BEP down below MCSF) for the key frequencies usually associated with internal hydraulic sources. In other words the new design impeller has the peculiar behavior to keep at low intensity in a wide operating range (and particularly at part flows) the internal flow mechanisms causing unsteady flows, which are susceptible of inducing pump structural vibrations (forced vibrations by hydraulic excitation).

At duty diameter the contractual performance requirements were achieved with the new impeller for each case with full acceptance by the customer. Moreover, the discharge recirculation was moved below the rated flow for all Cases and the margin above the suction recirculation onset capacity was further increased.

Field Vibration Data

Starting in June 2005 the new impellers were installed in all pumps (Case 1 to 4). The field vibrations and operations were in full compliance with specs meeting the customer's expectations in all four plants. Actual field vibrations are presented in Figures 23, 24 and 25 for Case 2 at the rated capacity of 3070 gpm ($N = 3580$ rpm, $SG = 0.56$) by comparing the last vibration data with the old impeller (17 March, 2005) and a series of vibration data with the new impeller (from 22 June, 2005 to 14 August, 2006). The overall vibration amplitude is compared in Figure 23, which shows that vibration level was exceeding the API limit of 0.12 ips for all radial components particularly at DEV and DEH. The new impeller has brought all vibration components within API limits with drastic reduction by a factor 3.5 of the highest values (DEV, DEH). Moreover the new vibration levels are consistently stable for more than a year of pump operation. The vibration at the synchronous frequency $1 \times$ rpm is compared in Figure 24: the pump with the original impeller presented higher vibration response at DEV-NDEV and much lower values for the other components, while the response with the new impeller was more even and in general low for all components. The vibration at $1 \times$ rpm can be related to both a mechanical unbalance of the impeller and also a hydraulic unbalance from casting deviation (e.g., blade angle at impeller outlet). It is hard to separate the two causes for interpreting this different vibration behavior. In principle it can be expected that an impeller with high vane number and lower vane loading (i.e., smaller pressure gradient at impeller outlet between the pressure side and the suction side of adjacent blades) is less sensitive to hydraulic balance due to geometry deviations.

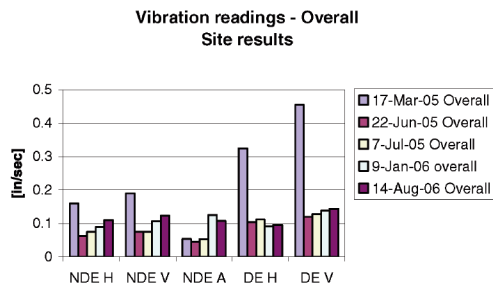


Figure 23. Field Data—Comparison—Overall (Case 2, $Q_{rated} = 3070$ GPM).

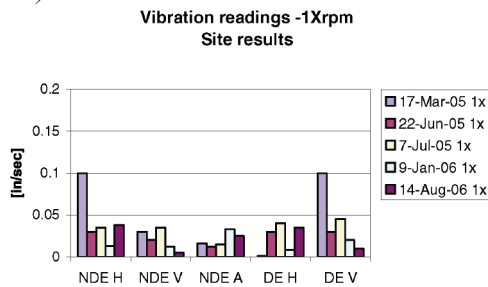


Figure 24. Field Data—Comparison— $1 \times$ RPM (Case 2, $Q_{rated} = 3070$ GPM).

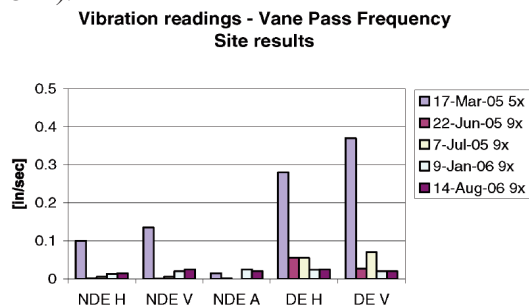


Figure 25. Field Data—Comparison—Vane Pass Frequency (Case 2, $Q_{rated} = 3070$ GPM).

In Figure 25 the comparison between the old and the new impeller is made for the key vibration frequency at vane pass with reference to the vane number at impeller outlet, where the largest fraction of the head generation takes place (i.e., five and nine vanes for old and new impeller, respectively). It is fully evident that the VPF radial vibrations at bearing housings are drastically reduced with the new impeller geometry by a factor 7 (at NDEV) up to 12 (at DEV) as exclusive effect of the hydraulic design optimization and innovative impeller geometry. It is worthy noticing that both the impellers have the same duty diameter with $D_{2duty} = 17.72$ inch and the same B gap = 16 percent, which is not playing any role in this drastic reduction of the VPF vibration. Then the reduction of the intensity of the hydraulic excitation forces as related with the impeller design appears as a primary factor for lowering the VPF vibrations. On the other hand the structural response of the bearing housings, which was not modified, has the highest natural frequencies (Table 2—second mode) below the VPF hydraulic excitation frequency (531 Hz). This is a second key factor contributing to the abatement of the VPF vibration.

One field vibration frequency spectrum with the new impeller for Case 2 (14 August, 2006) is shown in Figure 26 at the operating capacity of 2690 gpm (88 percent Q_{rated}) and 3580 rpm, $SG = 0.56$. The corresponding shop vibration frequency spectrum with the new impeller is shown in Figure 22 ($D_2 = 19.09$ inch, $SG = 1.0$). By comparison it appears that the drastic reduction of the VPF vibration is confirmed in the field also at this reduced capacity (refer to Figure 25 for 3070 gpm). However both the bandwidth of active frequencies is more enlarged up 1200 Hz (250 Hz in the shop test) and also the overall vibration level is increased (still remaining within the API limits) even with smaller diameter impeller ($D_{2duty} = 17.72$ inch) and lighter fluid ($SG = 0.56$). The most likely reason is that some degree of cavitation is present in the field as the ratio $NPSHA/NPSHR = 1.30$ (Table 1, Figure 3) is surely insufficient to eliminate cavitation at part flows with impeller eye peripheral velocity of 100 ft/s ($N = 3580$ rpm) (Schiavello, 1993).

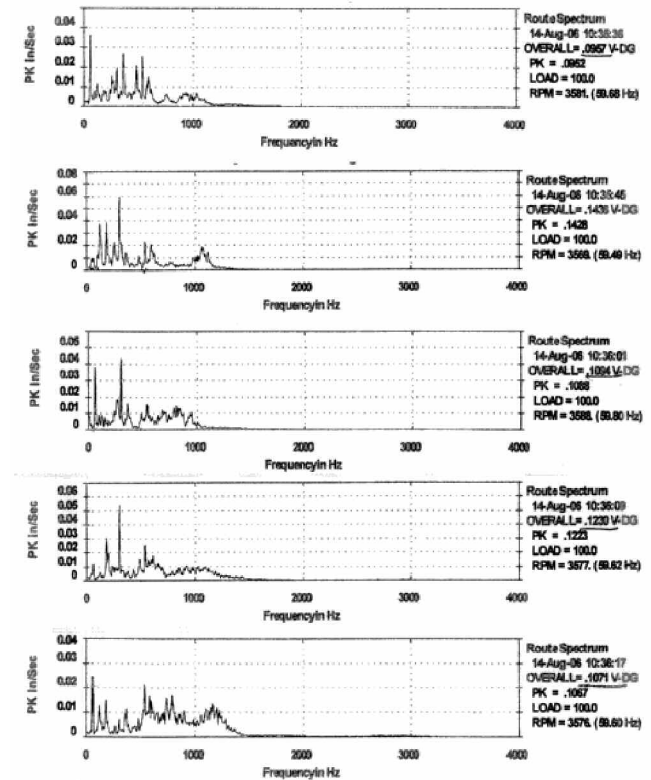


Figure 26. Field Test Spectra at 2690 GPM—New Impeller (Case 2).

CONCLUSIONS

The present paper illustrates an example of the importance of an analytical approach to the solution of a field problem.

Several pumps in various locations in the USA exhibited high vibrations above the API limits form rated point to MCSF. The investigation to identify the root cause was conducted along two independent paths, following precise and logical steps in line with an experimental and an analytical approach.

From the experimental point of view the steps were:

- Collect all available data from the field
- Comparison of field data with existing shop test data
- Reproduce the field conditions in terms of pump speed and operating conditions with a shop test
- Preliminary conclusions and first hypothesis
- Modal analysis to identify pump/bearing housing natural frequency
- Natural frequency manipulation through selective mass adding

From the analytical standpoint the hydraulic analysis has been conducted with the use of an extensive number of internal codes. It has certainly indicated that the root cause of the problem has to be associated with the discharge recirculation being well within the operating range of the pumps. The discharge recirculation triggering mechanism has been mainly associated with the impeller vanes design.

The attempts to manipulate the natural frequency of the pump by adding selective mass revealed to be only of limited advantage and appeared as a possible temporary measure due to the only partial results obtained.

A new design impeller was considered as the most effective solution strategy with high probability of success. The key points of the impeller design were mainly identified with:

- Delay the discharge recirculation onset capacity below the lowest rated flow
- Reduce the discharge recirculation strength
- Reduce vane loading by changing the impeller vanes number

To overtake the conflicting choices of the key design parameters an innovative impeller blade design was invoked with a double row of blades.

Shop tests revealed a drastic reduction of all vibration components below API acceptance level. Results were confirmed also in the field with full satisfaction of the customer.

NOMENCLATURE

BEP	= Best efficiency point
B gap	= Radial gap (volute cutwaters to impeller outlet) percent
D_{eye}	= Impeller eye diameter (inch)
D_2	= Impeller outer diameter (inch)
D_3	= Volute cutwater diameter (inch)
DE	= Drive end (inboard bearing housing)
DEH(V)	= Drive end horizontal (vertical)
H	= Head (ft)
ips	= Inch per second (vibration amplitude)
MCSF	= Minimum continuous stable flow (US gpm)
N	= Pump speed (rpm)
NDE	= Nondrive end (outboard bearing housing)
NDEA(H,V)	= Nondrive end axial (horizontal, vertical)
NPSHR	= Net positive suction head required for 3 percent head drop (HI definition) (ft)
NPSHA	= Net positive suction head available (ft)
NPSHinc	= Net positive suction head at cavitation inception (no vapor bubbles) (ft)

Ns	= Specific speed (rpm, Q_{total} - US gpm, ft)
Q	= Capacity (US gpm)
S_{eye}	= Suction specific speed (rpm, Q_{eye} - US gpm, ft)
SG	= Specific gravity
U_{eye}	= Peripheral velocity at impeller eye (ft/s)
VPF	= Vane passing frequency (Hz)
W	= Relative velocity (ft/s)
Z_2	= Impeller second row number of blades

Subscripts

actual	= Actual operating condition in the plant
BEP	= Best efficiency point at impeller outlet design diameter
BEPduty	= BEP at impeller outlet duty diameter (for rated point)
BEPmax	= BEP at impeller maximum outlet diameter
des	= Design
eye	= Impeller eye
inc	= Inception (no cavitation at all)
oper	= Operational
ps (ss)	= Impeller blade pressure (suction) side
rated	= Rated
rd	= Discharge recirculation
rs	= Suction recirculation

REFERENCES

- Barrand, J. P., Caignaert, G., Canavelis, R., and Guiton, P., 1984, "Experimental Determination of the Reverse Flow Onset in a Centrifugal Impeller," *Proceedings of the First International Pump Symposium*, Turbomachinery Laboratory, Texas A&M University, College Station, Texas, pp. 63-71.
- Bolleter, U., September 1988, "Blade Passages Tones of Centrifugal Pumps," *Vibrations*, 4, (3), pp. 8-13.
- Bolleter, U., Schwarz, D., Carney, B., and Gordon, E., 1991, "Solution to Cavitation Induced Vibration Problems in Crude Oil Pipeline Pumps," *Proceedings of the Eighth International Pump Users Symposium*, Turbomachinery Laboratory, Texas A&M University, College Station, Texas, pp. 21-27.
- Bruegelmans, F. A. E. and Sen, M., 1982, "Prerotation and Fluid Recirculation in the Suction Pipe of Centrifugal Pumps," *Proceedings of the Eleventh Turbomachinery Symposium*, Turbomachinery Laboratory, Texas A&M University, College Station, Texas, pp. 165-180.
- Cooper, P., Sloteman, P. D., Graf, E., and Vlaming, D. J., 1991, "Elimination of Cavitation-Related Instabilities and Damage in High-Energy Pump Impellers," *Proceedings of the Eighth International Pump Users Symposium*, Turbomachinery Laboratory, Texas A&M University, College Station, Texas, pp. 1-19.
- Dommm, H. and Hergt, P., 1970, "Radial Forces on Impeller of Volute Casing Pumps," *Flow Research on Bladings*, Dzung, L. S., ed., The Netherlands: Elsevier Publishing Co., pp. 305-321.
- Eisele, K., Zhang, Z., Casey, M. V., Gülich, J., and Schachenmann, A., 1997, "Flow Analysis in a Pump Diffuser—Part 1: LDA and PTV Measurements of the Unsteady Flow," *Transactions of the ASME, Journal of Fluids Engineering*, 119, pp. 968-977.
- Florjancic, S. S. and Frei, A., 1993, "Dynamic Loading on Pumps—Causes for Vibration," *Proceedings of the Tenth International Pump Users Symposium*, Turbomachinery Laboratory, Texas A&M University, College Station, Texas, pp. 171-184.
- Florjancic, S. S., Clothier, A. D., and Lopez Chavez, F. J., 1993, "A Case History—Improved Hydraulic Design Lowers Cavitation Erosion and Vibrations of a Water Transport Pump," *Proceedings of the Tenth International Pump Users Symposium*, Turbomachinery Laboratory, Texas A&M University, College Station, Texas, pp. 81-90.

- Fraser, W. H., 1981, "Flow Recirculation in Centrifugal Pumps," *Proceedings of the Tenth Turbomachinery Symposium*, Turbomachinery Laboratory, Texas A&M University, College Station, Texas, pp. 95-100.
- Gülich, J. F., 1989, "Guidelines for Prevention of Cavitation in Centrifugal Feedpumps," EPRI Research Project 1884-10, Final Report GS-6398.
- Gülich, J., Jud, W., and Hughes, S. F., 1987, "Review of Parameters Influencing Hydraulic Forces on Centrifugal Impellers," Seminar, "Radial Loads and Axial Thrusts on Centrifugal Pumps," Proc. Inst. Mech. Engrs., 201, (A3), London, United Kingdom, pp. 164-174.
- Gülich, J. F. and Bolleter, U., April 1992, "Pressure Pulsations in Centrifugal Pumps," *Transactions of the ASME, Journal of Vibrations and Acoustics*, 114, pp. 272-279.
- Hergt, P., and Starke, J., 1985, "Flow Patterns Causing Instabilities in the Performance of Centrifugal Pumps with Vaned Diffusers," *Proceedings of the Second International Pump Symposium*, Turbomachinery Laboratory, Department of Mechanical Engineering, Texas A&M University, College Station, Texas, pp. 67-75.
- Kanki, H., Kawata, J., and Kawatani, T., September 1981, "Experimental Research on Hydraulic Excitation Force on the Pump Shaft," ASME Design Technical Conference, ASME Paper No. 81-DET-71.
- Kaupert, K. A. and Staubli, T., 1999a, "The Unsteady Pressure Field in a High Specific Speed Centrifugal Pump Impeller—Part I: Influence of the Volute," *Transactions of ASME, Journal of Fluids Engineering*, pp. 621-626.
- Kaupert, K. A. and Staubli, T., 1999b, "The Unsteady Pressure Field in a High Specific Speed Centrifugal Pump Impeller—Part II: Transient Hysteresis in the Characteristics," *Transactions of ASME, Journal of Fluids Engineering*, pp. 627-632.
- Kawata, Y., Kanki, H., and Kawakami, T., 1984, "The Dynamic Radial Force on the Cavitating Centrifugal Impeller," *Proceedings of the Twelfth IAHR Symposium*, Stirling, United Kingdom, Paper 3.8, pp. 305-315.
- Kercan, V. and Schweiger, F., 1979, "Cavitation Phenomena Detection by Different Methods," *Proceedings of the Sixth Conference on Fluid Machinery*, Akademiai Kiado, Budapest, Hungary, pp. 535-543.
- Makay, E. and Barrett, J. A., 1984, "Changes in Hydraulic Component Geometries Greatly Increased Power Plant Availability and Reduced Maintenance Costs: Case Histories," *Proceedings of the First International Pump Symposium*, Turbomachinery Laboratory, Texas A&M University, College Station, Texas, pp. 85-100.
- Minami, S., Kawaguchi, K., and Homma, T., 1960, "Experimental Investigation on Cavitation in Centrifugal Pump Impellers," *Bulletin of JSME*, 3, (9), pp. 9-19.
- Okamura, T. and Miyashiro, H., 1978 "Cavitation in Centrifugal Pumps Operating at Low Capacities," Polyphase Flow in Turbomachinery, ASME Winter Annual Meeting, San Francisco, California, pp. 243-251.
- Robinett, F. L., Gülich, J. F., and Kaiser, T., 1999, "Vane Pass Vibration—Source, Assessment and Correction—A Practical Guide for Centrifugal Pumps," *Proceedings of the Sixteenth International Pump Users Symposium*, Turbomachinery Laboratory, Texas A&M University, College Station, Texas, pp. 121-138.
- Schiavello, B., 1982, "Critical Flow Engendering Appearance of Recirculation at Centrifugal Pump Impeller Inlet: Determinant Phenomena, Detection Methods, Forecasting Criteria," *La Houille Blanche*, 2/3, pp. 139-158 (in French).
- Schiavello, B., 1993, "Cavitation and Recirculation Troubleshooting Methodology," *Proceedings of the Tenth International Pump Users Symposium*, Turbomachinery Laboratory, Texas A&M University, College Station, Texas, pp. 133-156.
- Schiavello, B. and Sen, M., 1980, "On the Prediction of the Reverse Flow Onset at the Centrifugal Pump Inlet," *Proceedings of Performance Prediction of Centrifugal Pumps and Compressors*, ASME Twenty-Second Annual Fluids Engineering Conference, New Orleans, Louisiana, pp. 261-272.
- Schiavello, B. and Sen, M., 1981, "Experimental Investigation on Centrifugal Pump Design Criteria for Minimum Reverse Flow Delivery," Improvements in Turbomachines and Related Techniques, H. Worthington European Technical Award—1979, 5, Hoepli, Milan, Italy, pp. 191-239.
- Schiavello, B., Paton, A., and Rigamonti, G., 1997, "Pump Impeller Having Separate Offset Inlet Vanes," US Patent Number: 5,605,444.
- Sen, M., Breugelmans, F. A. E., and Schiavello, B., 1979, "Reverse Flow, Prerotation and Unsteady Flows in Centrifugal Pumps," *Proceedings of Fluid Mechanic Silver Jubilee Conference*, Paper No. 3.1, National England Laboratory, East Kilbride, Glasgow, United Kingdom.
- Sloteman, D. P., Cooper, P., and Dussourd, J. L., 1984, "Control of Backflow at the Inlets of Centrifugal Pumps and Inducers," *Proceedings of the First International Pump Symposium*, Turbomachinery Laboratory, Texas A&M University, College Station, Texas, pp. 9-22.
- Timouchev, S. and Turret, J., 2002, "Numerical Simulation of BPF Pressure Pulsation Field in Centrifugal Pumps," *Proceedings of the Nineteenth International Pump Users Symposium*, Turbomachinery Laboratory, Texas A&M University, College Station, Texas, pp. 85-106.
- Verhoeven, J. J., 1987, "Unsteady Hydraulic Forces in Centrifugal Pumps," *Conference on Partload Pumping, Proc. Inst. Mech. Engrs.*, 201, (A3), Edinburgh, Scotland, pp. 163-174.
- Verhoeven, J. J., 1988, "Rotordynamic Considerations in the Design of High Speed, Multistage Centrifugal Pumps," *Proceedings of the Fifth International Pump Users Symposium*, Turbomachinery Laboratory, Texas A&M University, College Station, Texas, pp. 81-92.
- Worster, R. C., 1960, "The Interaction of Impeller and Volute in Determining the Performance of a Centrifugal Pump," The British Hydromechanics Research Association, RR 679.
- Worster, R. C., 1963, "The Flow in Volutes and its Effect on Centrifugal Pump Performance," *Proceedings of the I. Mech. E.*, 177, (31), London, United Kingdom, pp. 341- 376.

ACKNOWLEDGEMENTS

The authors would like to thank the management of Flowserve Corporation, USA, and Flowserve Italy for permission to publish this paper. The authors are especially grateful to Azfar Ali of Flowserve Technology Department for his contribution to hydraulic analysis.

